Lithology and climate controlled soil aggregate size distribution and organic carbon stability in the Peruvian Andes

Songyu Yang [1], Boris Jansen [1], Samira Absalah [1], Rutger van Hall [1], Karsten Kalbitz [2], Erik Cammeraat [1]

1 Institute for Biodiversity and Ecosystem Dynamics, University of Amsterdam, Amsterdam, Netherlands

2 Soil Resources and Land Use, Institute of Soil Science and Site Ecology, Technische Universität Dresden, Dresden, Germany

Correspondence to: Songyu Yang (s.yang@uva.nl; longxianfeijian@163.com)

Abstract

Recent studies indicate that climate change influences soil mineralogy by altering weathering processes, and thus impacts soil aggregation and organic carbon (SOC) stability. Alpine ecosystems of the Neotropical Andes are characterized by high SOC stocks, which are important to sustain ecosystem services. However, climate change in the form of altered precipitation patterns can potentially affect soil aggregation and SOC stability with potentially significant effects on the soil's ecosystem services. This study aimed to investigate the effects of precipitation and lithology on soil aggregation and SOC stability in the Peruvian Andean grasslands, and assessed whether occlusion of organic matter (OM) in aggregates controls SOC stability. For this, samples were collected from soils on limestone and soils on acid igneous rocks from two sites with contrasting precipitation levels. We used a dry-sieving method to quantify aggregate size distribution, and applied a 76-day soil incubation with intact and crushed aggregates to investigate SOC stability in dependence on aggregation. SOC stocks ranged from 153±27 to 405±42 Mg ha^{-1}, and the highest stocks were found in the limestone soils of the wet site. We found lithology rather than precipitation to be the key factor regulating soil aggregate size distribution, as indicated by coarse aggregates in the limestone soils and fine aggregates in the acid igneous rock soils. SOC stability estimated by specific SOC mineralization rates decreased with precipitation in the limestone soils, but minor differences were found between wet and dry sites in the acid igneous rock soils. Aggregate destruction had a limited effect on SOC mineralization, which indicates that occlusion of OM in aggregates played a minor role in OM stabilization. This was further supported by the inconsistent patterns of aggregate size distribution compared to the patterns of SOC stability. We propose that OM adsorption on mineral surfaces is the major OM stabilization mechanism controlling SOC stocks and stability. The results highlight the interactions between precipitation and lithology on SOC stability, which are likely controlled by soil mineralogy in relation to OM input.

Keywords: soil organic matter; stabilization; precipitation; limestone; acid igneous rock; aggregate destruction

1 Introduction

Soil organic carbon (SOC) is the largest terrestrial carbon (C) pool and plays an important role in global C dynamics (Carvalhais et al., 2014; Lal, 2004). However, the distribution of SOC at a global scale is highly variable (Batjes, 2014; Lal, 2004). Alpine grasslands of the Andes are characterized by large SOC stocks,

especially for the Ecuadorian and Peruvian Andes (Muñoz García and Faz Cano, 2012; Rolando et al., 2017a; Tonneijck et al., 2010). The Andean grasslands play a crucial role in agricultural production, water provision and sustaining the high biodiversity (Buytaert et al., 2011; Rolando et al., 2017a). The large SOC stocks contribute to crucial ecosystem services, and act as a potential C sink or source for atmospheric CO_2 in the context of global change (Buytaert et al., 2011). However, the studied region, the Andes in Northern Peru, is characterized by heterogeneity in climate, vegetation, agricultural activities and geological formations (Buytaert et al., 2006b; Rolando et al., 2017a), which potentially introduces spatial variability in SOC storage and stability.

Recent views on SOC persistence have shifted from chemical recalcitrance of soil organic matter (OM) to progressive decomposition of soil OM dependent on the surrounding biotic and abiotic environment (Lehmann and Kleber, 2015; Schmidt et al., 2011). Specifically, SOC persistence and stabilization are controlled by: (1) OM adsorption on mineral surfaces that controls long-term stabilization, and (2) physical occlusion of OM within soil aggregates that regulates intermediate-term stabilization with heterogeneous OM composition and residential time (Lützow et al., 2006; Schrumpf et al., 2013). Adsorption of OM on mineral surfaces was reported as an important stabilization mechanism for soil OM underlying the large SOC stocks in the Peruvian and Ecuadorian Andes (Buytaert *et al.*, 2006a; Tonneijck *et al.*, 2010; Yang *et al.*, submitted). However, studies focusing on aggregate-controlled OM stabilization in relation to climate in the Andes are rare (e.g. Rolando *et al.*, 2017b). Aggregates promote soil OM stabilization against decomposition by regulating the availability of oxygen and water as well as the accessibility of OM itself (Kong et al., 2005). Thus, the formation and turnover of soil aggregates are crucial for SOC storage and OM stabilization (Six et al., 2004; Six and Paustian, 2014). As soil aggregates are formed with monomers of clay minerals, polyvalent cations and OM, their formation and the underlying OM stabilization largely depend on various biotic and abiotic factors (e.g. climate and lithology) (Bronick and Lal, 2005; Doetterl et al., 2015).

Lithology is the key factor controlling soil OM stabilization and soil aggregation, mainly attributed to its controls on soil mineralogy and texture (Angst et al., 2018; Homann et al., 2007; Wiesmeier et al., 2019). In soils formed on acidic bedrocks, OM is generally considered to be stabilized by ligand exchange with non-crystalline Fe and Al oxides, whereas in soils formed on alkaline-rich bedrocks, OM is thought to be stabilized by interaction with the mineral surface through polyvalent cation bridges (e.g. Ca^{2+}) (Lützow et al., 2006). Soil texture also has effects on OM stabilization because OM-mineral association is dominantly controlled by clay-sized minerals (Kaiser and Guggenberger, 2003; Kleber et al., 2007). In addition, soil mineralogy and texture are crucial factors for soil aggregation (Bronick and Lal, 2005). In soils developed on base-rich or calcareous materials, the high clay and calcium (Ca) contents promote the

formation of large-sized aggregates. In soils developed on sand-rich or acidic materials, the lack of alkaline cations (e.g. Ca^{2+}) and the coarse texture hinder the formation of coarse aggregates (Bronick and Lal, 2005; Six et al., 2004). The differences in aggregation can potentially affect soil OM stabilization as controlled by occlusion of OM within aggregates (Lützow et al., 2006).

Climate factors, comprising temperature and precipitation, act as the primary drivers regulating SOC storage and OM stabilization by controlling OM input and decomposition (Schmidt et al., 2011; Wiesmeier et al., 2019). Recent studies indicated that climate factors also control OM persistence by regulating soil mineralogy (Chaplot et al., 2010; Doetterl et al., 2015, 2018). The soil mineralogy and OM persistence controlled by climate can be dependent on lithology due to their inherent properties (Jenny, 1994; Wagai et al., 2008). Given the importance of climate and lithology, the heterogeneity in precipitation and lithology in the Andes can potentially cause spatial variation in OM stabilization and consequently SOC stocks. In addition, shifts in e.g. precipitation patterns as a result of global change may impact SOC stocks in different parts of the Andes in different ways.

The objectives of our study were to assess the controls of precipitation and lithology on SOC stocks and stability in the Peruvian Andes. Specifically, we aimed to investigate whether the effects of precipitation and lithology on SOC stability are through the controls of OM stabilization governed by aggregate occlusion and/or mineral adsorption. For this, we applied a combination of aggregate-size fractionation with a 76-day incubation for soil samples collected from the Peruvian Andes with two contrasting bedrocks and two precipitation levels.

2 Materials and methods

2.1 Site description

Basic information of the sampling sites is shown in Fig. 1. The study areas belong to the Neotropical alpine grassland of the Andes, corresponding to the grassland ecosystem commonly referred as wet Puna or Jalca that is present between the tree line (3500 m asl) and the ice-covered region, having an annual precipitation over 500 mm (Rolando et al., 2017a). Two sampling sites were selected with similar altitudes but with different lithologies and precipitation levels. The wet site is located in the western Cordillera mountain chain of the Peruvian Andes, to the west of Cajamarca, Peru (7°11` S, 78°35` W). The altitudes of the sites range from 3500 m to 3720 m asl. The temperature shows a large daily variation and minor seasonal variation, with an estimated annual mean of 11°C. The sites receive 1100mm precipitation per year and have a wet season between October and April (Sánchez Vega et al., 2005). The

dry site is located in the mountain chain of the Cordillera Blanca, to the northeast of Carhuaz (9°22` S, 77°59` W), with altitudes ranging between 3490 and 3700 m asl. The annual temperature and precipitation were estimated as 11 °C and 680 mm, and had similar annual and daily variations as the wet site (Merkel, 2017). Typical land use in both sites is grassland with human activities including cultivation, grazing and plantation of pine trees and eucalyptus (Rolando et al., 2017a; Sánchez Vega et al., 2005). The vegetation in the wet site is a typical disturbed wet Puna (or Jalca) vegetation with dominant grass species *Calamagrostis sp.*, but also *Festuca and Agrostis sp. as well as Rumex sp.* on fallow land. Similarly, the vegetation in the dry site is also a typical disturbed wet Puna (or Jalca) vegetation with *Calamogrostis sp., Stipa and Festuca sp. and Rumex sp.* on fallow land.

For the wet site, the geology consists of a basement of Cretaceous sedimentary formations, which is composed of limestone, marl, shale and quartzite. Neogene igneous bedrocks consisting of granite and ignimbrite intrude or cover parts of the basement (Reyes-Rivera, 1980). For the dry site, intrusive igneous rocks (mainly granodiorite) belonging to the Neogene Cordillera Blanca batholith are present in the western part of the Cordillera Blanca (Coldwell et al., 2011; Portes et al., 2016). The foot slopes consist of fluvio-glacial and glacial sediments partly covering andesitic ignimbritic rocks of the Neogene Yungay formation, as well as the sedimentary Cretaceous Carhuaz and Santa formations that are dominated by folded limestones, sandstones and shales (Coldwell et al., 2011). Soils developed on the limestone were classified as Phaeozems or Umbrisols, whereas soils on acid igneous rocks were classified as Andosols and Umbrisols (WRB, 2014).

2.2 Sampling procedures

For both the wet and dry sites, we selected three soil sampling plots from limestone and three plots on acid igneous rocks. For limestone soils (LSs) in both sites and acid igneous rock soils (ASs) in the wet site, all soils were directly developed on the bedrock. For ASs in the dry site, one sampling site was directly developed on granodiorite, whereas the other two sites were located on the glacier deposits on lateral moraines with a granodioritic composition. As a previous study in the study area showed that SOC stocks are not significantly controlled by land use (Yang et al., 2018), all sampling sites were selected based on the criteria of (1) grassland, grassland with shrubs or abandoned cropland, (2) gentle slopes, (3) no intensive human activities, and (4) similar soil development status.

For the determination of bulk density and calculation of SOC stocks through the soil profile, samples were collected every 10 cm in duplicate to the depth of the C horizon using Kopecky rings (100 cm^3). For the determination of basic soil properties, aggregate-size fractionation and incubation, soil samples were

collected per horizon in triplicate (e.g. A_{h1}, A_{h2} and B_{tg} horizons). To minimize aggregate destruction during transportation, soil samples were transferred into sealed plastic bags and protected by hard plastic boxes.

2.3 Laboratory analyses

Soil samples collected every 10 cm were freeze-dried to determine bulk densities and SOC stocks. Soil bulk densities were measured by weighing samples after freeze-drying. Afterward, gravels (>2 mm) were removed from the samples. The rest of the samples was used to determine OC contents and to calculate SOC stocks. Soil samples collected per horizon were air-dried, followed by taking 5-10 g of sub-samples milled for the determination of basic soil properties. For these samples, total C and N contents were analyzed using a VarioEL Elementar analyzer (Elementar, Germany). As inorganic C contents were negligible in all the samples, the total OC contents were equal to total C contents. Soil pH was determined with a glass electrode in suspensions of soil material in demi-water (w:v=1:5, Bates, 1973).

Total SOC stocks were calculated using the following equation:

$$SOC\ stock = \sum_{i=1}^{i=k} BD_i \times C_i \times (1 - S_i) \times D_i$$

In which, BD_i = bulk density (g cm^{-3}) of the layer i (including gravels), C_i = SOC content (%) of the layer i (excluding gravels), S_i = stoniness (gravimetric) of layer i, D_i= thickness (cm) of layer i.

Dry-sieving was applied to fractionate soil samples into 5 aggregate-size groups: >5mm, 2-5mm, 0.22-2 mm, 0.063-0.25 mm and <0.063 mm, respectively. Briefly, 170-230 g sub-samples (<16 mm) of each horizon were fractionated using 4 mesh sieves (5, 2, 0.25 and 0.063 mm) by shaking for 20 s at 30 Hz at a horizontal shaker. For all fractions larger than 2 mm, gravels were separated by sieving (2 mm) a subsample of the fraction after breaking aggregates. The gravel content (gravimetric) of each fraction was calculated using the gravel weight divided by the sum of the fraction weight plus the gravel weight. For each fraction, fraction weights as well as total C and N contents were determined.

The mean weight diameter (MWD) of the bulk soil was calculated by:

$$MWD = \sum_{i=1}^{i=5} \frac{x_{i\,max} + x_{i\,min}}{2} \times w_i$$

In which, $x_{i\,max}$ = maximum diameter (mm) of the fraction i, $x_{i\,min}$ = minimum diameter (mm) of the fraction i, w_i = weight percent (excluding gravels) of the fraction i (Klute and Dinauer, 1986).

Sample materials collected from different horizons were used for the incubation. All materials from individual A horizons in the same soil profile were merged (e.g. Ah1 and Ah2 horizons merged to A horizon), based on the weight distribution of the horizons as estimated by their bulk densities and depths. Original B horizons were used because each soil profile only had a single B horizon. Prior to the incubation, all samples were fractionated into large macroaggregates (LM, > 2mm), small macroaggregates (SM, 0.25-2 mm) and microaggregates (Mi, <0.25 mm), following the dry-sieving procedure (30 Hz for 20 s). The LM and SM fractions were used for the incubation with intact and crushed aggregates. The finer fractions (<0.25 mm) were by far less abundant, and thus were not incubated. The variation in SOC mineralization between intact and crushed aggregates was used as a measure of C stabilization by occlusion within aggregates (Goebel et al., 2009). Aggregates were destructed by crushing the fractions using a porcelain mortar, and all crushed materials could pass a 0.125 mm sieve (Wang et al., 2014). Before incubation, intact and crushed fractions were rewetted at pF 2.0 for 10 days to activate soil microbes. Approximate 10 g dry-weight equivalent fractions were incubated for 76 days at 20 °C in sealed glass jars (120 ml). All soil fractions were incubated in duplicate. The headspace of incubating jars was sampled on days 1, 2, 6, 9, 13, 20, 28, 48 and 76. During the sampling period, CO_2-free air was injected into the jars to maintain pressure and avoid too high CO_2 concentrations. The CO_2 concentration was analyzed using a gas chromatograph with a flame ionization detector (GC-FID, Thermo Scientific, Trace GC Ultra) with packed columns (RESTEK Packed Column, Part Nbr: PC7130, Serial Nbr: C34216-01, HayeSep Q, 1/8" 80/100 2m and HayeSep Q, 1/8" 80/100 1m). A methanizer was situated in front of the FID, as the detector can only measure hydrocarbons instead of CO_2. Specific SOC mineralization rates (g CO_2-C g^{-1} C), which were normalized for OC contents, were used as an indicator of the C stability of the soil fractions.

2.4 Statistics

Statistical comparisons of soil properties and SOC stocks were made using a one-way ANOVA. *Post hoc* analyses were conducted using the Fisher's Least Significant Difference (LSD) test. Principal component analysis (PCA) was applied to investigate potential differences between different soil profiles and horizons. Before conducting the PCA, Kaiser-Meyer-Olkin tests and Bartlett's tests were used to guarantee that sampling adequacy and the sphericity were suitable for the analysis. Linear regressions were applied to investigate relationships of specific SOC mineralization rates with SOC and C/N ratios.

An independent *t*-test was applied to check effects of precipitation, lithology, soil horizon, aggregate size and aggregates destruction on SOC mineralization rates.

Before the *t*-test and the one-way ANOVA, data normality and variance homogeneity were examined using a Shapiro-Wilk test and a Levene's test. When the assumption of normality was violated, the Kruskal-Wallis H test was applied instead of the one-way ANOVA, while the Mann-Whitney U-test was used instead of the *t*-test. When the homogeneity of the variance could not be assumed, the Robust Welch test was used for the one-way ANOVA. All analyses were conducted using SPSS 24.0 (SPSS Inc., USA).

3 Results

3.1 Soil properties

Average soil depths were 61cm for limestone soils (LSs) in both wet and dry sites, and 49 cm and 51 cm for acid igneous rock soils (ASs) in the wet and the dry sites (Fig. 1). SOC stocks were highest in LSs of the wet site (wet-LSs, 405.3 ± 41.7 Mg ha^{-1}), followed by ASs of the wet site (wet-ASs), ASs of the dry site (dry-ASs) and dry-LSs. SOC stocks in the wet-LSs were significantly higher compared to other soils (Fig. 2). SOC contents in the A horizons were significantly higher in the wet-LSs both with regard to bedrock and precipitation. No significant differences were present for the ASs with regard to precipitation (Fig. 2). The LSs had no significant difference in C/N ratios compared to the ASs for the A horizons in the wet sites, however, the LSs had significantly lower C/N ratios in the dry site (Fig. 2). With decreasing precipitation, C/N ratios significantly decreased in the LSs and increased in the ASs (Fig. 2). pH values were significantly higher in the LSs compared to the ASs in the wet site, but were not significantly different in the dry site (Fig. 2). In addition, significantly lower pH values with lower precipitation were only found in the LSs (Fig. 2). With regard to the differences between horizons in the LSs, B horizons were characterized by significant lower SOC contents, lower C/N ratios and higher pH compared to A horizons, except for SOC contents and pH values in the dry sites (Fig. 2).

3.2 Aggregate-size fractionation

The weight distribution of the aggregate-size fractions is shown in Fig 3A and 3C. The LSs had larger aggregate sizes than the ASs in both wet and dry sites, as indicated by that LSs had more LM fraction (> 60%) and less Mi fraction (< 10%) when compared to the AS (Fig 3A and 3C). When comparing the wet and dry sites, the aggregate-size distribution was not clearly different in the LSs. In contrast, the wet-ASs

had larger aggregate sizes (more LM fraction) than the dry-ASs (Fig. 3A and 3C). When comparing the A and B horizons in the LSs, B horizons had larger aggregates sizes compared to A horizons for both wet-LSs and dry-LS (Fig. 3A and 3C). The SOC distribution in different fractions is similar to the weight distribution as shown in Fig. 3B and 3D. The LSs had more SOC located in large-sized aggregates than the ASs , whereas the wet-ASs had more SOC distributed in large aggregates than the dry-ASs. For the LSs, B horizons had more SOC distributed in large-sized aggregates when compared to A horizons (Fig 3A-3D).

Soil properties of different horizons are shown in Fig. 4. PC1 and PC2 explained 67.0 % and 17.9 % of the total variation. PC1 had positive contributions of the SM and Mi fractions and negative loadings of the LM fractions and MWD, whereas PC2 had positive contributions of C and N contents. The LSs were separated from the ASs as indicated by coarser aggregates, higher pH values and lower C/N ratios (Fig. 4). In addition, wet-LSs were separated from dry-LSs by higher C and N contents, whereas ASs were not clearly separated by precipitation (Fig. 4). The LSs were characterized by increasing coarse aggregate fractions and decreasing C and N contents as well as C/N ratios with increasing soil depth, whereas the ASs had no clear pattern in soil property change with increasing depth (Fig. 4).

3.3 SOC mineralization

After the 76-day incubation, specific SOC mineralization rates were the highest in A and B horizons of the dry-LSs, when compared to the other soil horizons (Fig. 5A-5D). For comparisons between two lithologies, SOC mineralization rates were not significantly different in the wet site, but were generally higher in the LSs compared to the ASs in A horizons of the dry site (Table 1). For effects of precipitation, SOC mineralization rates were significantly higher in the dry site compared to the wet site for the LS-A horizons in most sampling days, but were not significantly different for the AS-A horizons (Table 1). For comparisons between A and B horizons in the LSs, SOC mineralization rates were not significantly different in the wet site. In the dry site, A horizons had significantly higher SOC mineralization rates than B horizons only in the aggregate-crushed SM fraction (Table 1).

SOC mineralization rates were slightly stimulated (up to 19.4 %) when aggregates were crushed compared to that when aggregates were intact, with exceptions of the LM fraction in dry-AS-A horizons and the SM fraction in dry-AS-A horizons and wet-LS-A horizons (Fig 6A and 6B). However, the stimulation caused by aggregate destruction was never significant (Fig. 6A and 6B). In addition, no significant difference in SOC mineralization rates was found between LM and SM fractions. Exclusively,

slightly higher SOC mineralization rates (not significant) were found in the SM fraction compared to LM fraction in A horizons of the wet-LS, the dry-LSs and the dry-ASs (Fig. 6C and 6D).

Overall, SOC mineralization rates had significant negative relationships with SOC contents and C/N ratios, and the negative relationships did not differ between intact and crushed aggregates (Fig. 7A and 7B). Exclusively for the dry-LSs, positive relationships were found between SOC mineralization rates and SOC contents when aggregates were intact and crushed, and between SOC mineralization rates and C/N ratios when aggregates were crushed (Fig. 7C-7F). In the dry-LSs, SOC contents and C/N ratios explained 38.2 % and 24.9 % of the variation of specific SOC mineralization rates when aggregates were intact. When aggregates were crushed, SOC contents and C/N ratios explained 48.0 % and 33.3 % of the total variation (Fig. 7C-7F).

4 Discussion

4.1 Aggregate size distribution

Lithology is the key factor controlling soil aggregate-size distribution in our soils, as indicated by larger aggregates in the LSs when compared to the ASs (Fig. 3). The larger aggregates in the LSs are consistent with the literature (Bronick and Lal, 2005; Six et al., 2004). The lithology-controlled aggregate-size distribution can be further supported by the physicochemical properties of aggregate fractions (Fig. S1). Compared to the LSs, the ASs had higher C/N ratios in all fractions than the LSs and had a larger increase in OC contents with decreasing fraction size when aggregate size was smaller than 2 mm (Fig. S1). Furthermore, increasing aggregate sizes with soil depth were found in the LSs exclusively (Fig. 4), which can be explained by the better aggregation promoted by clay illuviation in deep soils. In contrast, no clear vertical differences in the ASs may be related to the lack of the clay fraction in the ASs (Yang *et al.*, submitted).

Unlike lithology, precipitation plays only a minor role in the soil aggregate size distribution for our soils. This is indicated by small differences in properties related to soil aggregation between the wet and the dry sites for the same bedrock types (Fig. 3, Fig. 4 and Fig. S1). Although precipitation potentially controls the OM input and further affects soil aggregation (Bronick and Lal, 2005, Wiesmeier et al., 2019), similar vegetation between wet and dry sites (see *2.1 site description*) might alleviate the controls of precipitation on OM input and soil aggregation. In addition, the effects of precipitation might be superimposed by the strong effect of lithology in our study.

Notably, the dry-ASs had smaller aggregates than the wet-ASs (Fig. 3). This is probably attributed to their greater gravel contents in the dry-ASs (Fig. 1 and Table S1) because abundant gravels occupy the space and hinder the formation of large-sized aggregates. Furthermore, gravel contents may affect soil aggregation by controlling root distribution, OM input or soil biological activity. The greater gravel contents in the dry-ASs are likely to be attributed to the terrain conditions (steep mountains and glacial deposits) rather than precipitation (Portes *et al.* 2016). Although aggregate-size distribution is controlled by gavel contents, the physicochemical properties of each aggregate fraction were not clearly affected. This is corroborated by: (1) no clear differences in vertical distribution of aggregate-related soil properties between wet-ASs and dry-ASs (Fig. 4), and (2) no clear differences in properties of aggregate fractions between wet-ASs and dry-ASs (Fig. S1). An important reason for this is that gravels were always removed from all fractions >2 mm. Thus, analyses conducted for aggregates fractions (e.g. SOC mineralization) are not biased by gravel contents.

4.2 SOC stocks and stability

SOC stocks were controlled by interactions between lithology and precipitation, as indicated by increased stocks with precipitation in the LSs and no significant changes in the ASs (Fig. 2). Lithology had significant effects on SOC stocks in the wet sites (Fig. 2), which is consistent with the findings of Yang *et al.* (2018) showing that lithology is the key factor controlling SOC stocks. In the wet site, the high SOC stocks in the LSs compared to the ASs can be explained by deeper soils and higher SOC contents in A horizons (Fig. 1 and 2). In the dry site, no difference in SOC stocks between the LSs and the ASs can be explained by that the LSs had lower SOC contents but deeper profiles (Fig. 1 and 2). Precipitation had significant effects on SOC stocks of the LSs, as indicated by the wet-LSs having greater SOC stocks than the dry-LSs (Fig. 2). This is consistent with the consensus that SOC stocks generally increase with precipitation (Homann et al., 2007; Wiesmeier et al., 2019). The higher SOC stocks in the wet-LSs can be also explained by SOC contents because of (1) similar soil depths in the wet-LSs and the dry-LSs (Fig. 1) and (2) lower soil bulk densities in the wet-LSs (Table S2). Hence, patterns of SOC stocks controlled by lithology and precipitation are mainly explained by SOC contents.

The negative correlations between SOC contents and SOC mineralization rates (Fig. 7A and 7B) reflect SOC contents controlled by SOC stability. The SOC stability is significantly controlled by precipitation and lithology (Table 1) rather than soil horizon, aggregate size or aggregate destruction (Fig. 6). For horizons, although SOC stability was different between A and B horizons in the crushed SM fraction of

the dry-LSs (Table 1), the small contribution of the SM fraction (Fig. 3) suggests that horizon is not an important factor controlling the SOC stability.

320

4.3 Organic matter stabilization mechanisms

SOC stability is largely controlled by two mechanisms: (1) OM adsorption on the mineral surfaces and (2) physical occlusion of OM within soil water-stable aggregates (Lützow et al., 2006; Six et al., 2002). In general, OM occluded in water-stable aggregates is isolated using wet-sieving followed by density
325 fractionation plus sonication (Cerli et al., 2012; Moni et al., 2012). However, these methods were not applicable for our ASs because the application of ultrasound caused severe dispersion of OM into the dense solution (i.e. NaPT). The dispersed OM was difficult to be separated from the solution and thus occluded OM could not be isolated. A similar situation has been reported and a potential explanation is that Na^+ in the solution interacted with Al-OM complexes in the ASs and produced a stable suspension
330 (Kaiser and Guggenberger 2007). As the problem could not be solved, we applied an alternative method, which has been conducted by Goebel et al. (2009) and Wang et al. (2014), to estimate aggregate-occluded OM using a combination of dry-sieving and incubating intact versus crushed aggregates.

Overall, aggregate-occlusion is not a major OM stabilization mechanism in our soils, as indicated by no or insignificant stimulation in SOC mineralization after aggregate destruction (Fig. 6). The minor role of
335 aggregate-occlusion is further supported by the minor changes in correlation patterns of SOC mineralization rates with SOC contents and C/N ratios, when aggregates were intact and crushed (Fig. 7A and 7B). The limited effects of OM occlusion in aggregates are not consistent with the general view of aggregate-controlled OM stabilization (Lehmann and Kleber, 2015; Wiesmeier et al., 2019), as well as other studies revealing aggregate-protected OM using similar aggregate destruction methods (Mueller et
340 al., 2012; Wang et al., 2014). However, Goebel *et al.* (2009) and Juarez *et al.* (2013) reported limited roles of soil aggregates in protecting OM from decomposition. For the ASs, the limited role of aggregates-occlusion in OM stabilization can be explained by the lack of large-sized aggregates (Fig. 3), which suggests the restricted formation of microaggregates within macroaggregates. This potentially weakens the OM protection controlled by occlusion in aggregates (Six et al., 2002; Six and Paustian,
345 2014). For the LSs, the minor contribution of aggregates might be related to the strong adsorption of OM on less-saturated mineral surfaces (Yang *et al.*, submitted). Because of the limited contribution of OM occlusion in aggregates, OM adsorption on mineral surfaces is most likely the dominant stabilization mechanism. Similar to our results, mineral-controlled OM stabilization mechanisms have been reported in

other studies in alpine grassland soils of the Andes (Yang *et al.*, submitted; Buytaert *et al.*, 2006a; Tonneijck *et al.*, 2010; Rolando *et al.*, 2017b).

Lithology is an important factor for OM stabilization related to mineral surfaces. Yang *et al.* (submitted) found that OM stabilization in the wet-LSs was controlled by OM complexed and/or adsorbed with Fe and Al (oxides) as well as by Ca^{2+} bridges. In contrast, OM stabilization in the wet-ASs was only controlled by Fe and Al (oxides) complexation (Yang *et al.* submitted). In the wet site, SOC stability between LSs and ASs was not significantly different (Table 1). This may be attributed to the mineral surfaces in both LSs and ASs having a large capability for OM stabilization, although their OM stabilization mechanisms are slightly different. In the dry site, lower SOC stability in the LSs compared to the ASs (Table 1) suggests the lower capacity of the mineral surfaces to stabilize OM in the LSs. Similarly, Heckman *et al.* (2009) found lower SOC stocks and stability in LSs compared to soils formed on felsic and basaltic igneous rocks, in a region with similar temperature and precipitation to our dry site. They explained this by a lack of active Fe and Al fractions to stabilize OM (Heckman et al., 2009), which might be an explanation for the less stable SOC in our dry-LSs as well.

Precipitation is also an important factor to explain the low SOC stability in the dry-LSs, as precipitation has a potential effect on soil mineralogy by controlling weathering processes (Doetterl et al., 2015, 2018; Wiesmeier et al., 2019). Compared to the wet-LSs, the lower pH values in the dry-LSs indicate that a part of exchangeable base cations (e.g Ca^{2+}) are replaced by exchangeable H^+. The replacement results in lower adsorption capacity of the mineral surfaces because H^+ is a monovalent cation that does not promote OM stabilization (Jenny, 1994; Lützow et al., 2006). In addition, positive correlations between SOC mineralization rates and SOC contents, and between SOC mineralization and C/N ratios in the dry-LSs (Fig. 7) indicate that SOC mineralization is dominantly dependent on SOC contents and quality. This also suggests a lower sorption capacity of the mineral adsorption sites. Similarly, Wagai *et al.* (2008) reported positive correlations between SOC mineralization and C/N ratios, and used the positive correlations as an indication of inert mineral surfaces. Furthermore, the lowest C/N ratios in the dry-LSs (Fig. 2) indicate a depletion of plant-derived C and a rapid SOC decomposition process (Moni et al., 2012), which suggests the low SOC stability and the low capacity of mineral surfaces to stabilize OM.

4.4 Interactions between precipitation and lithology

The effects of precipitation and lithology on SOC stocks and stability are unlikely through the controls of soil aggregation, which is supported by the weak controls of OM stabilization via occlusion in aggregates

(Fig. 6 and 7) and inconsistent patterns of aggregate size distribution compared to the patterns of SOC stability (Fig. 3, Fig. 4 and Table 1). In contrast, the interactions between precipitation and lithology on SOC stocks and stability are likely explained by soil mineralogy. This is supported by (1) the contrasting OM stabilization mechanisms controlled mineral surfaces between the wet-LS and the wet-AS (Yang *et al.*, submitted), and (2) shifts in pH values, C/N ratios and correlations between SOC mineralization rates and SOC contents that suggest variations in properties of the mineral surfaces (Fig. 2 and Fig. 7).

Recent studies indicate that controls of climate factors and soil mineralogy are crucial to the persistence and stabilization of soil OM (Chaplot et al., 2010; Doetterl et al., 2015; Homann et al., 2007). For the LSs, we proposed that the lower SOC stability in the dry site is explained by the weaker interactions between OM and mineral surfaces due to the lower pH when compared to the wet site. However, the lower pH in the dry-LSs is not consistent with the general soil formation process. The lower pH in the dry-LSs might be explained by soil acidification induced by higher belowground OM input compared to the wet-LSs. The higher OM input in the dry-LSs is supported by (1) more abundant α, ω-dioic acids, ω-hydroxyl alkanoic acids and long-chain fatty acids, especially in B horizons (Fig. S2), and (2) low stability of these compounds against decomposition in the dry-LSs (Fig. S3). As these compounds are mainly derived from root input (Kögel-Knabner, 2002), the lower pH in the dry-LSs can be explained by the higher belowground OM input because plants need more developed root systems for the low precipitation. By contrast, no clear difference is found between the wet-ASs and the dry-ASs (Fig. 1 and Table 1). This may be attributed to the limited acidification induced by OM input because the bedrocks are already acidic. Notably, our statement on OM input is based on estimation because quantification of OM input in Andean grasslands is difficult and only a few studies have addressed this (Oliveras et al., 2014).

Similar to our results, Wagai et al. (2008) reported that the controls of altitude (temperature and precipitation) on OM stoichiometry (indicating mineral surface activity) are dependent on soil bedrocks. Furthermore, Doetterl et al. (2015, 2018) indicated that climate factors in relation to soil mineralogy control the potential of soil matrix to stabilize OM. Our findings also support their views that the OM persistence is controlled by climate factors and soil mineralogy. We further propose that the interactions between precipitation and lithology on OM stabilization in our study are through the controls of soil mineralogy in relation to OM input.

5 Conclusion

Our findings highlighted (1) SOC stocks and stability controlled by interactions between precipitation and lithology, and (2) soil aggregate size distribution controlled by lithology only. We did not find an important effect of precipitation on aggregation, which was probably superimposed by the effect of lithology. As the assumption that aggregate occlusion contributes to OM stabilization is not supported by our data, we conclude that OM adsorption on mineral surfaces is the major OM stabilization mechanism in these soils. We propose that the controls of precipitation and lithology on SOC stocks and OM stabilization are through the controls of soil mineralogy in relation to OM input.

Further studies are required for more lithology types and more precipitation levels. In addition, primary effects of precipitation on OM dynamics are not limited to the controls of soil mineralogy. Potential effects of precipitation on quantity and quality of input OM suggest that investigations in OM molecular composition may contribute to a better understanding of the processes governing SOC sequestration in the Neotropical grasslands of the Andes.

Author contribution. SY, BJ, KK and EC conceived and designed the study; RvH contributed to the experiments related to aggregate-size fractionation and analyses of soil properties; SA contributed to the soil incubation and the SOC mineralization measurement; SY wrote the paper. All authors contributed to the manuscript revision.

Competing interests. The authors declare that they have no conflict of interest.

Acknowledgement. We thank Lisa Boerdam, Chiara Cerli and Eva de Rijke for their help in lab work, as well as Xiang Wang for sharing his experiences for the incubation experiment. We thank Fresia Olinda Chunga Castro for her assistant in the field sampling. We also thank the Mountain Institute (TMI) for their support in the field work, and Institute for Biodiversity and Ecosystem Dynamics (IBED) and China Scholarship Council (CSC) for funding.

Reference

Angst, G., Messinger, J., Greiner, M., Häusler, W., Hertel, D., Kirfel, K., Kögel-Knabner, I., Leuschner, C., Rethemeyer, J. and Mueller, C. W.: Soil organic carbon stocks in topsoil and subsoil controlled by

parent material, carbon input in the rhizosphere, and microbial-derived compounds, Soil Biol. Biochem., 122(July 2017), 19–30, doi:10.1016/j.soilbio.2018.03.026, 2018.

Bates, R. G.: Determination of pH: theory and practice, J. Electrochem. Soc., 120(8), 3C–263C, 1973.

Batjes, N. H.: Total carbon and nitrogen in the soils of the world, Eur. J. Soil Sci., 65(1), 1, doi:10.1111/ejss.12120, 2014.

Boix-Fayos, C., Calvo-Cases, A., Imeson, A. C. and Soriano-Soto, M. D.: Influence of soil properties on the aggregation of some Mediterranean soils and the use of aggregate size and stability as land degradation indicators, Catena, 44(1), 47–67, doi:10.1016/S0341-8162(00)00176-4, 2001.

Bronick, C. J. and Lal, R.: Soil structure and management: a review, Geoderma, 124(1–2), 3–22, doi:10.1016/j.geoderma.2004.03.005, 2005.

Buytaert, W., Deckers, J. and Wyseure, G.: Description and classification of nonallophanic Andosols in south Ecuadorian alpine grasslands (páramo), Geomorphology, 73(3–4), 207–221, doi:10.1016/j.geomorph.2005.06.012, 2006a.

Buytaert, W., Celleri, R., Willems, P., Bièvre, B. De and Wyseure, G.: Spatial and temporal rainfall variability in mountainous areas: A case study from the south Ecuadorian Andes, J. Hydrol., 329(3–4), 413–421, doi:10.1016/j.jhydrol.2006.02.031, 2006b.

Buytaert, W., Cuesta-Camacho, F. and Tobón, C.: Potential impacts of climate change on the environmental services of humid tropical alpine regions, Glob. Ecol. Biogeogr., 20(1), 19–33, doi:10.1111/j.1466-8238.2010.00585.x, 2011.

Carvalhais, N., Forkel, M., Khomik, M., Bellarby, J., Jung, M., Migliavacca, M., Mu, M., Saatchi, S., Santoro, M., Thurner, M., Weber, U., Ahrens, B., Beer, C., Cescatti, A., Randerson, J. T., Reichstein, M., Mu, M., Saatchi, S., Santoro, M., Thurner, M., Weber, U., Ahrens, B., Beer, C., Cescatti, A., Randerson, J. T., Reichstein, M., Mu, M., Saatchi, S., Santoro, M., Thurner, M., Weber, U., Ahrens, B., Beer, C., Cescatti, A., Randerson, J. T. and Reichstein, M.: Global covariation of carbon turnover times with climate in terrestrial ecosystems, Nature, 514, 213–217, doi:10.1038/nature13731, 2014.

Cerli, C., Celi, L., Kalbitz, K., Guggenberger, G. and Kaiser, K.: Separation of light and heavy organic matter fractions in soil — Testing for proper density cut-off and dispersion level, Geoderma, 170, 403–416, doi:10.1016/j.geoderma.2011.10.009, 2012.

Chaplot, V., Bouahom, B. and Valentin, C.: Soil organic carbon stocks in Laos: Spatial variations and

controlling factors, Glob. Chang. Biol., 16(4), 1380–1393, doi:10.1111/j.1365-2486.2009.02013.x, 2010.

Coldwell, B., Clemens, J. and Petford, N.: Deep crustal melting in the Peruvian Andes: Felsic magma generation during delamination and uplift, Lithos, 125(1–2), 272–286, doi:10.1016/j.lithos.2011.02.011, 2011.

Doetterl, S., Stevens, A., Six, J., Merckx, R., Oost, K. Van, Pinto, M. C., Casanova-katny, A., Muñoz, C., Boudin, M., Venegas, E. Z. and Boeckx, P.: Soil carbon storage controlled by interactions between geochemistry and climate, Nat. Geosci., 8(10), 780–783, doi:10.1038/NGEO2516, 2015.

Doetterl, S., Berhe, A. A., Arnold, C., Bodé, S., Fiener, P., Finke, P., Fuchslueger, L., Griepentrog, M., Harden, J. W., Nadeu, E., Schnecker, J., Six, J., Trumbore, S., Van Oost, K., Vogel, C. and Boeckx, P.: Links among warming, carbon and microbial dynamics mediated by soil mineral weathering, Nat. Geosci., 11(8), 589–593, doi:10.1038/s41561-018-0168-7, 2018.

Esri. "Topographic" [basemap]. Scale Not Given. "World Topographic Map". June, 2013. http://www.arcgis.com/home/item.html?id=30e5fe3149c34df1ba922e6f5bbf808f. (June, 2019).

GEO GPS PERÚ, 2014. “GEO GPS PERÚ: Base De Datos Perú - Shapefile - *.Shp - MINAM - IGN - Límites Políticos.”, https://www.geogpsperu.com/2014/03/base-de-datos-peru-shapefile-shp-minam.html.

Goebel, M. O., Woche, S. K. and Bachmann, J.: Do soil aggregates really protect encapsulated organic matter against microbial decomposition?, Biologia (Bratisl)., 64(3), 443–448, doi:10.2478/s11756-009-0065-z, 2009.

Heckman, K., Welty-Bernard, A., Rasmussen, C. and Schwartz, E.: Geologic controls of soil carbon cycling and microbial dynamics in temperate conifer forests, Chem. Geol., 267(1–2), 12–23, doi:10.1016/j.chemgeo.2009.01.004, 2009.

Homann, P. S., Kapchinske, J. S. and Boyce, A.: Relations of mineral-soil C and N to climate and texture: Regional differences within the conterminous USA, Biogeochemistry, 85(3), 303–316, doi:10.1007/s10533-007-9139-6, 2007.

Jenny, H.: Factors of soil formation: a system of quantitative pedology, Courier Corporation., 1994.

Juarez, S., Nunan, N., Duday, A. C., Pouteau, V., Schmidt, S., Hapca, S., Falconer, R., Otten, W. and Chenu, C.: Effects of different soil structures on the decomposition of native andadded organic carbon, Eur. J. Soil Biol., 58, 81–90, doi:10.1016/j.ejsobi.2013.06.005, 2013.

Kaiser, K. and Guggenberger, G.: Distribution of hydrous aluminium and iron over density fractions depends on organic matter load and ultrasonic dispersion, Geoderma, 140(1–2), 140–146, doi:10.1016/j.geoderma.2007.03.018, 2007.

Kaiser, K. and Guggenberger, G.: Mineral surfaces and soil organic matter, Eur. J. Soil Sci., 54(2), 219–236, doi:10.1046/j.1365-2389.2003.00544.x, 2003.

Kleber, M., Sollins, P. and Sutton, R.: A conceptual model of organo-mineral interactions in soils: self-assembly of organic molecular fragments into zonal structures on mineral surfaces, Biogeochemistry, 85(1), 9–24, doi:10.1007/s10533-007-9103-5, 2007.

Klute, A. and Dinauer, R. C.: Methods of Soil Analysis Part 1. Physical and Mineralogical Methods, 2nd ed., edited by A. Klute, Madison., 1986.

Kögel-Knabner, I.: The macromolecular organic composition of plant and microbial residues as inputs to soil organic matter: Fourteen years on, Soil Biol. Biochem., 34(2), 139–162, doi:10.1016/S0038-0717(01)00158-4, 2002.

Kong, A. Y. Y., Six, J., Bryant, D. C., Denison, R. F. and van Kessel, C.: The Relationship between Carbon Input, Aggregation, and Soil Organic Carbon Stabilization in Sustainable Cropping Systems, Soil Sci. Soc. Am. J., 69(4), 1078, doi:10.2136/sssaj2004.0215, 2005.

Lal, R.: Soil carbon sequestration impacts on global climate change and food security, Science (80-.)., 304(5677), 1623–1627 [online] Available from: //000221934300036, 2004.

Lehmann, J. and Kleber, M.: The contentious nature of soil organic matter., Nature, 528(7580), 60–8, doi:10.1038/nature16069, 2015.

Lützow, M. V., Kögel-Knabner, I., Ekschmitt, K., Matzner, E., Guggenberger, G., Marschner, B. and Flessa, H.: Stabilization of organic matter in temperate soils: mechanisms and their relevance under different soil conditions - a review, Eur. J. Soil Sci., 57(4), 426–445, doi:10.1111/j.1365-2389.2006.00809.x, 2006.

Merkel, A.: Climate-data, [online] Available from: https://en.climate-data.org/south-america/peru-27/, 2017.

Moni, C., Derrien, D., Hatton, P.-J., Zeller, B. and Kleber, M.: Density fractions versus size separates: does physical fractionation isolate functional soil compartments?, Biogeosciences, 9(12), 5181–5197, doi:10.5194/bg-9-5181-2012, 2012.

Mueller, C. W., Schlund, S., Prietzel, J., Kögel-Knabner, I. and Gutsch, M.: Soil Aggregate Destruction by Ultrasonication Increases Soil Organic Matter Mineralization and Mobility, Soil Sci. Soc. Am. J., 76(5), 1634, doi:10.2136/sssaj2011.0186, 2012.

Muñoz García, M. A. and Faz Cano, A.: Soil organic matter stocks and quality at high altitude grasslands of Apolobamba, Bolivia, Catena, 94, 26–35, doi:10.1016/j.catena.2011.06.007, 2012.

Portes, R. D. C., Spinola, D. N., Reis, J. S., Ker, J. C., Costa, L. M. Da, Fernandes Filho, E. I., Kühn, P. and Schaefer, C. E. G. R.: Pedogenesis across a climatic gradient in tropical high mountains, Cordillera Blanca - Peruvian Andes, Catena, 147, 441–452, doi:10.1016/j.catena.2016.07.027, 2016.

Reyes-Rivera, L.: Geología de los cuadrángulos de Cajamarca, San Marcos y Cajambamba 15-f, 15-g, 16-g-[Boletín A 31]., 1980.

Rolando, J. L., Turin, C., Ramírez, D. A., Mares, V., Monerris, J. and Quiroz, R.: Key ecosystem services and ecological intensification of agriculture in the tropical high-Andean Puna as affected by land-use and climate changes, Agric. Ecosyst. Environ., 236, 221–233, doi:10.1016/j.agee.2016.12.010, 2017a.

Rolando, J. L., Dubeux, J. C., Perez, W., Ramirez, D. A., Turin, C., Ruiz-Moreno, M., Comerford, N. B., Mares, V., Garcia, S. and Quiroz, R.: Soil organic carbon stocks and fractionation under different land uses in the Peruvian high-Andean Puna, Geoderma, 307(March), 65–72, doi:10.1016/j.geoderma.2017.07.037, 2017b.

Sánchez Vega, I., Cabanillas Soriano, M., Miranda Leiva, A., Poma Rojas, W., Díaz Navarro, J. and Terrones Hernández, F Bazán Zurita, H.: La jalca: el ecosistema frio del noroeste peruano, fundamentos biologicos y ecologicos., 2005.

Schmidt, M. W. I., Torn, M. S., Abiven, S., Dittmar, T., Guggenberger, G., Janssens, I. A., Kleber, M., Kögel-Knabner, I., Lehmann, J., Manning, D. A. C., Nannipieri, P., Rasse, D. P., Weiner, S. and Trumbore, S. E.: Persistence of soil organic matter as an ecosystem property., Nature, 478(7367), 49–56, doi:10.1038/nature10386, 2011.

Schrumpf, M., Kaiser, K., Guggenberger, G., Persson, T., Kögel-Knabner, I. and Schulze, E.-D.: Storage and stability of organic carbon in soils as related to depth, occlusion within aggregates, and attachment to minerals, Biogeosciences, 10(3), 1675–1691, doi:10.5194/bg-10-1675-2013, 2013.

Six, J. and Paustian, K.: Aggregate-associated soil organic matter as an ecosystem property and a measurement tool, Soil Biol. Biochem., 68, A4–A9, doi:10.1016/j.soilbio.2013.06.014, 2014.

Six, J., Conant, R. T., Paul, E. A. and Paustian, K.: Stabilization mechanisms of soil organic matter : Implications for C-saturation of soils, , 155–176, 2002.

Six, J., Bossuyt, H., Degryze, S. and Denef, K.: A history of research on the link between (micro)aggregates, soil biota, and soil organic matter dynamics, Soil Tillage Res., 79(1), 7–31, doi:10.1016/j.still.2004.03.008, 2004.

Tonneijck, F. H., Jansen, B., Nierop, K. G. J., Verstraten, J. M., Sevink, J. and De Lange, L.: Towards understanding of carbon stocks and stabilization in volcanic ash soils in natural Andean ecosystems of northern Ecuador, Eur. J. Soil Sci., 61(3), 392–405, doi:10.1111/j.1365-2389.2010.01241.x, 2010.

Wagai, R., Mayer, L. M., Kitayama, K. and Knicker, H.: Climate and parent material controls on organic matter storage in surface soils: A three-pool, density-separation approach, Geoderma, 147(1–2), 23–33, doi:10.1016/j.geoderma.2008.07.010, 2008.

Wang, X., Cammeraat, E. L. H., Cerli, C. and Kalbitz, K.: Soil aggregation and the stabilization of organic carbon as affected by erosion and deposition, Soil Biol. Biochem., 72, 55–65, doi:10.1016/j.soilbio.2014.01.018, 2014.

Wiesmeier, M., Urbanski, L., Hobley, E., Lang, B., von Lützow, M., Marin-Spiotta, E., van Wesemael, B., Rabot, E., Ließ, M., Garcia-Franco, N., Wollschläger, U., Vogel, H. J. and Kögel-Knabner, I.: Soil organic carbon storage as a key function of soils - A review of drivers and indicators at various scales, Geoderma, 333(July 2018), 149–162, doi:10.1016/j.geoderma.2018.07.026, 2019.

WRB, I. W. G.: World reference base for soil resources 2014. International soil classification system for naming soils and creating legends for soil maps, FAO, Rome., 2014.

Yang, S., Cammeraat, E., Jansen, B., den Hann, M., van Loon, E. and Recharte, J.: Soil organic carbon stocks controlled by lithology and soil depth in a Peruvian alpine grassland of the Andes, Catena, 171(June), 11–21, doi:10.1016/j.catena.2018.06.038, 2018.

Yang, S., Jansen, B., Kalbitz, K., Chunga Castro, F. O., van Hall, R. L. and Cammeraat, E. L. H.: Lithology controlled soil organic carbon stabilization in an alpine grassland of the Peruvian Andes, Submitt to Environ. Earth Sci.

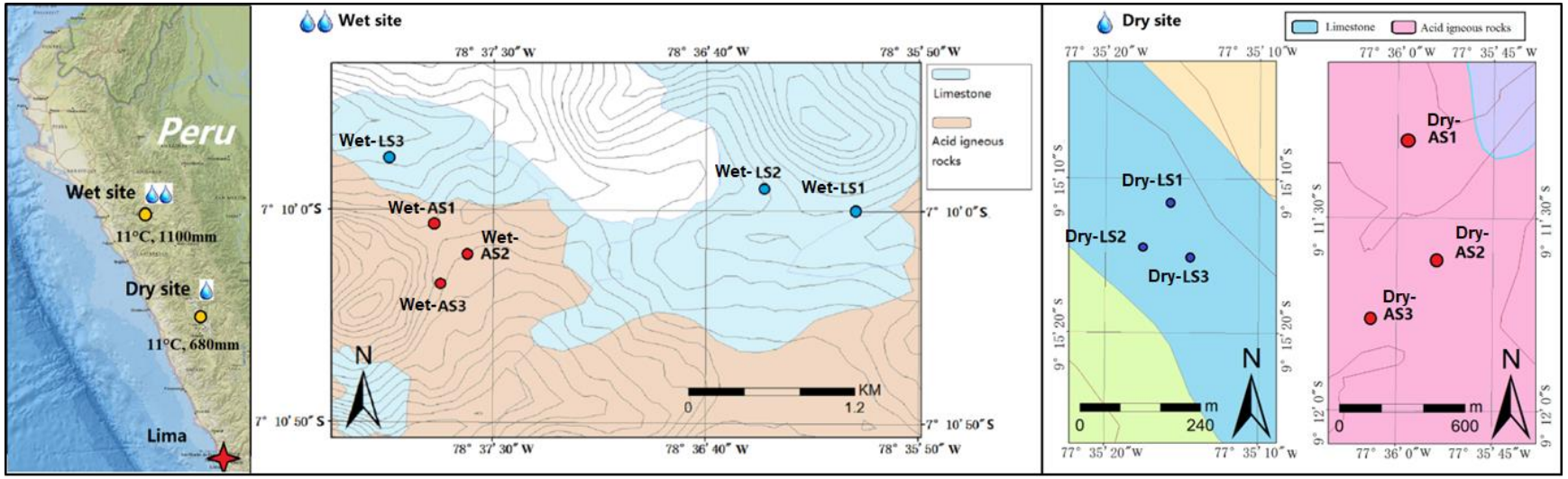

Site	Wet site					Dry site				
	Parent material	Altitude	Soil depth	Ave. depth	Gravels in LM fractions	Parent material	Altitude	Soil depth	Ave. depth	Gravels in LM fractions
		m	cm		%		m	cm		%
LS1	Limestone	3716	57		6.86	Limestone	3573	56		8.70
LS2	Limestone	3717	66	61	3.13	Limestone	3532	54	61	5.42
LS3	Limestone	3517	60		0.16	Limestone	3560	73		13.01
AS1	Granite/ignimbrite	3583	68		10.86	Granodiorite	3667	44		50.28
AS2	Granite/ignimbrite	3585	45	49	14.12	Granodiorite-rich glacier materials	3521	60	51	39.57
AS3	Granite/ignimbrite	3586	35		28.60	Granodiorite-rich glacier materials	3495	50		61.05

Fig. 1 Sampling site description. LS: limestone soil, AS: acid igneous rock soil, LM: large macroaggregates (>2 mm). The ArcGIS Online World Topographic Map basemap (Esri., 2013) was used for the map of Peru on the left, whereas the data for the contour lines in the maps of the wet site and the dry site was derived from Geo GPS Perú, (2014).

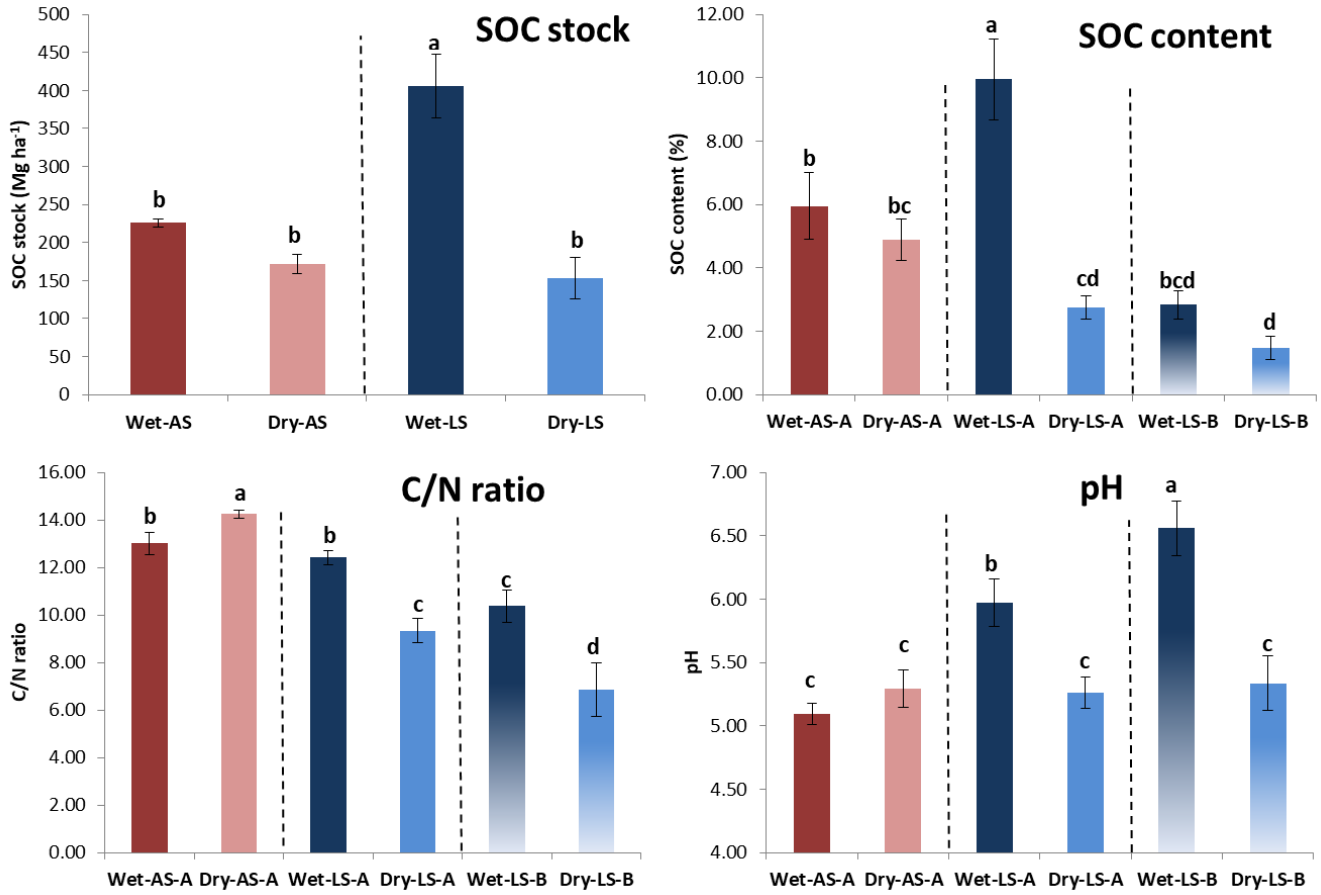

Fig. 2 Soil organic carbon stocks in the whole soil profile and soil properties in diagnostic horizons (Mean±SE). Wet: the wet site, Dry: the dry site, LS: limestone soil, AS: acid igneous rock soil, A: A horizons, B: B horizons

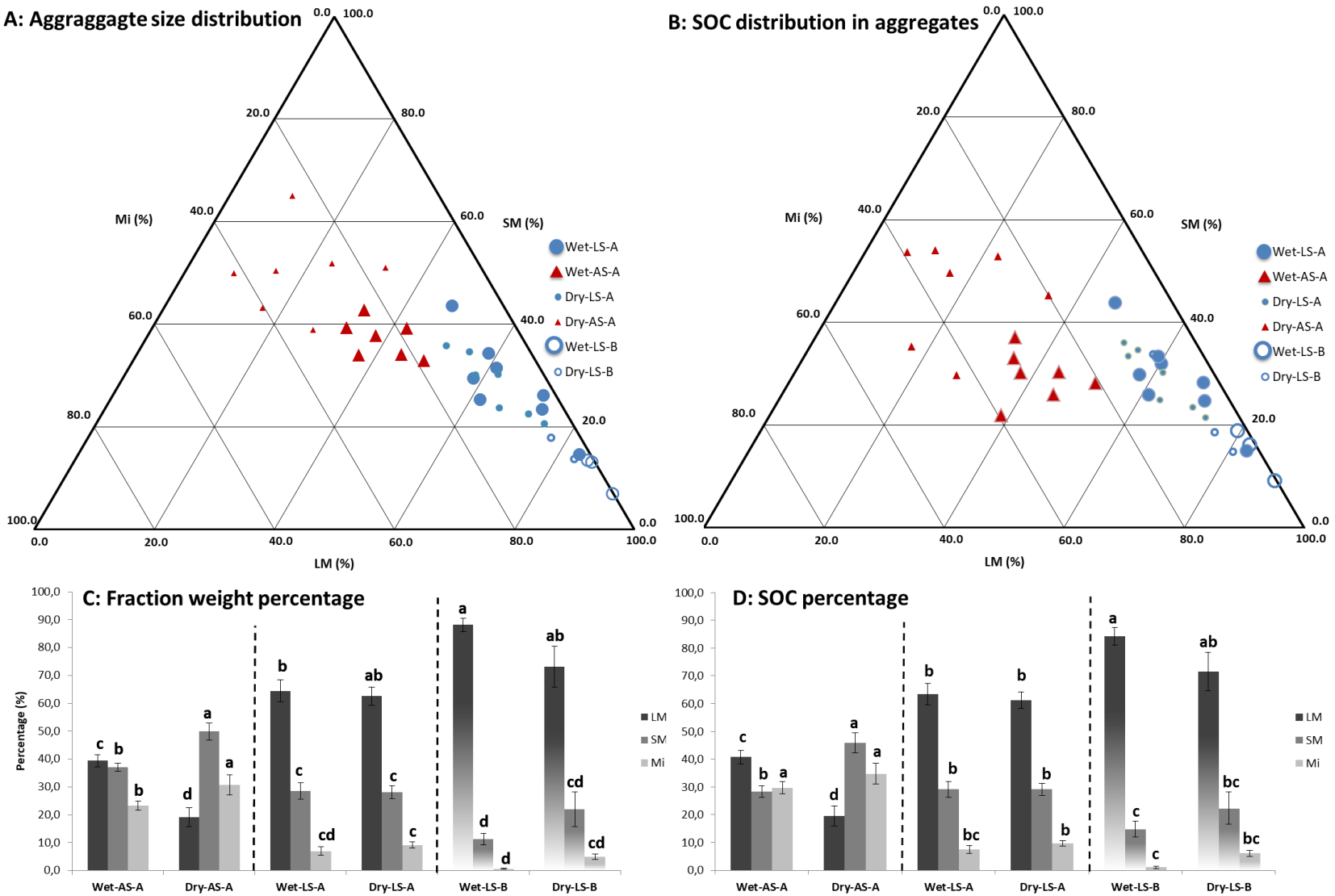

Fig. 3 Distribution of fraction weight and soil organic carbon in aggregate size fractions. A: Fraction weight distribution in aggregate size fractions, B: SOC distribution in aggregate size fractions, C: percentages of fraction weights in soil horizons (Mean±SE), D: SOC percentage in soil horizons (Mean±SE). Wet: the wet site, Dry: the dry site, LS: limestone soil, AS: acid igneous rock soil, A: A horizons, B: B horizons, LM: large macroaggregates (>2 mm), SM: small macroaggregates (0.25-2 mm), Mi: microaggreagtes (<0.25 mm)

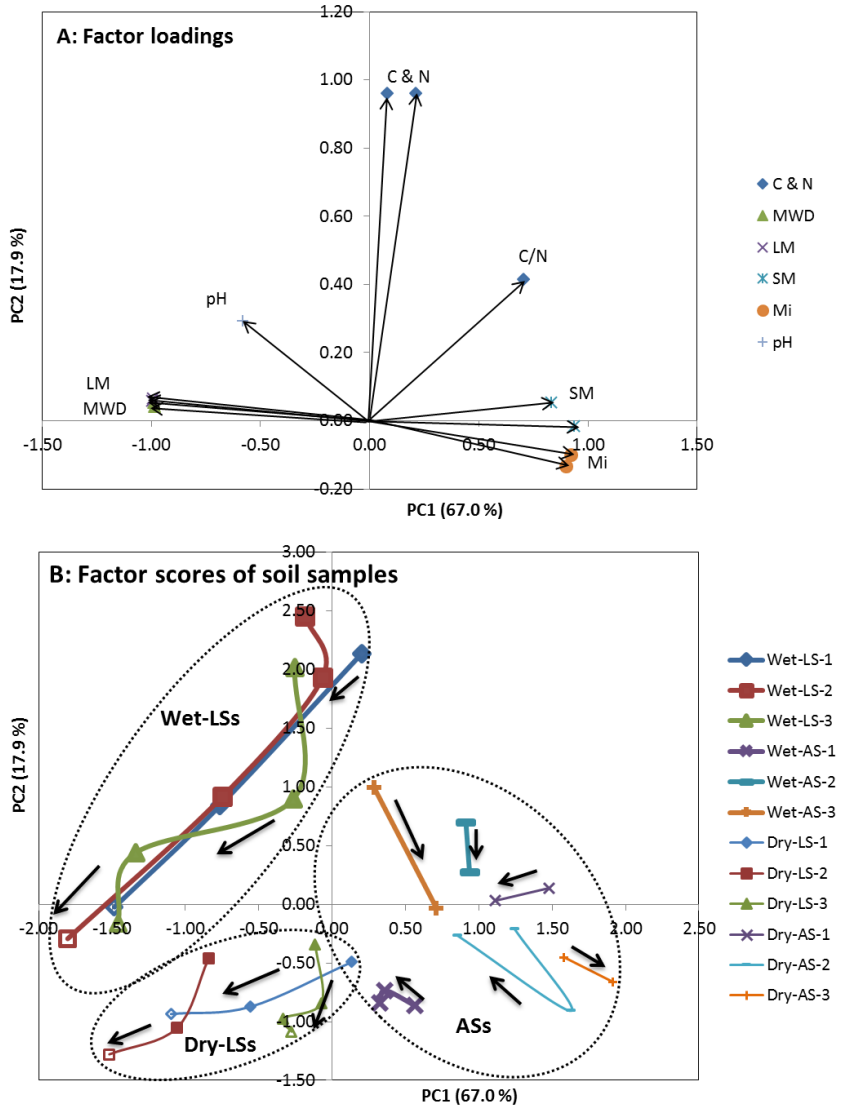

Fig. 4 Principal component analysis (PCA) indicating vertical distribution of aggregate-related soil properties in both limestone soils (LSs) and acid igneous rock soils (ASs). Solid points are A horizons, and hollow points are B horizons. Black arrows are pointing to the direction of soil horizons with increasing soil depth. Wet: the wet site, Dry: the dry site, LS: limestone soil, AS: acid igneous rock soil, MWD: mean weight diameter, C: SOC content, N: total nitrogen content, C/N: C/N ratio, LM: large macroaggregates, SM: small macroaggregates, Mi: microaggregates.

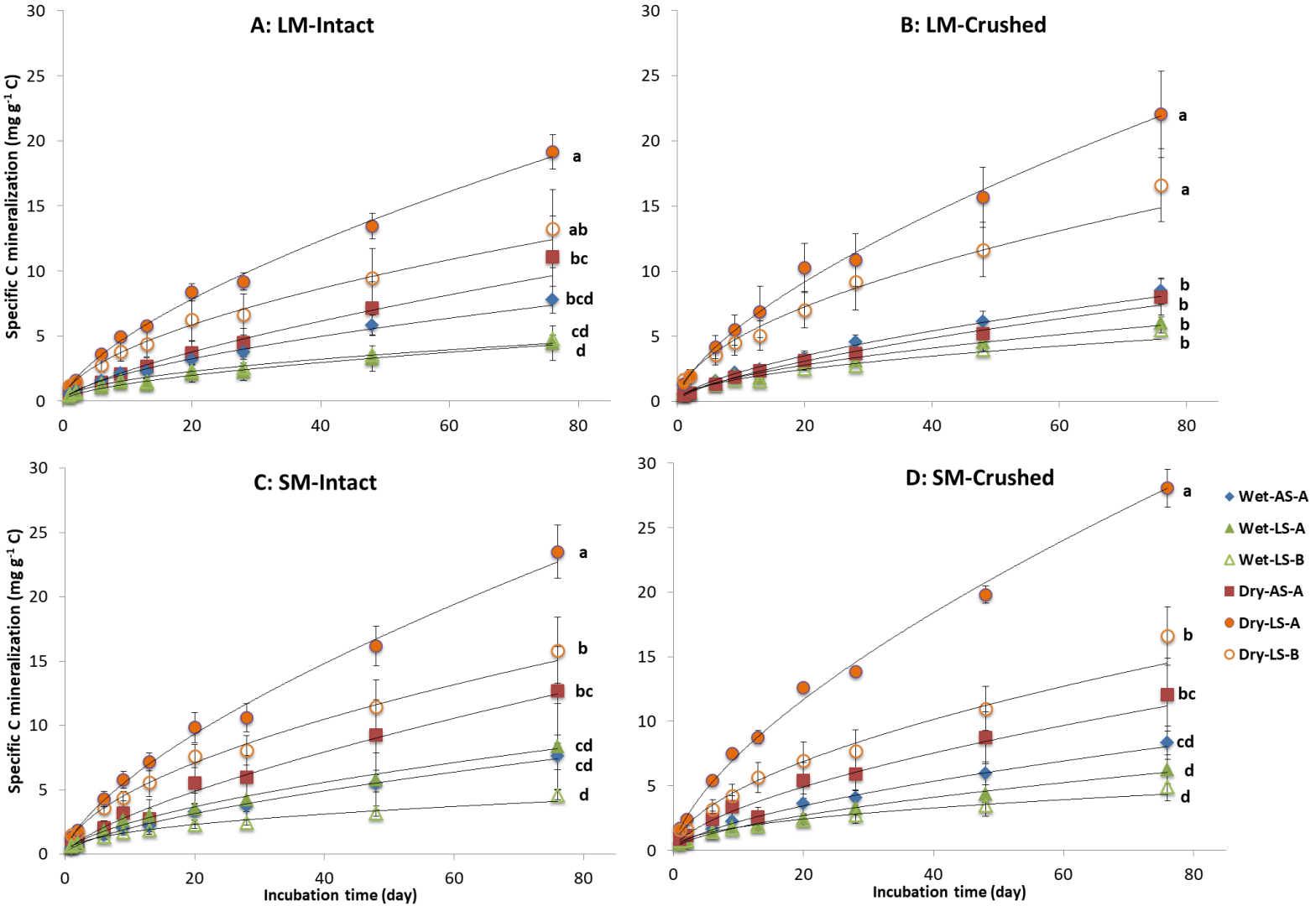

Fig. 5 SOC mineralization in the large macroaggregats (LM) and small macroaggregates (SM) in a period of 76-day incubation, with aggregate intact and crushed (Mean ± SE). Letters on the right of each plots indicate significant differences of cumulative C mineralization between different groups on Day 76. LM: large macroaggregates (>2 mm), SM: small macroaggregates (0.25-2 mm), Intact: incubation with aggregates intact, Crushed: incubation with aggregates crushed, Wet: the wet site, Dry: the dry site, AS-A: acid igneous rock soil - A horizon, LS-A: limestone soil - A horizon, LS-B: limestone soil - B horizon.

Table 1 Comparison in SOC mineralization rates between bedrock, precipitation and horizon with combinations of aggregate sizes and aggregate destruction. Abbreviations in the table indicating the group with significant higher SOC mineralization than the other group.

	A horizon: LS vs. AS				**A horizon: Wet vs. Dry**				**LS: A vs. B horizon**			
	LM-In	**LM-Cr**	**SM-In**	**SM-Cr**	**LM-In**	**LM-Cr**	**SM-In**	**SM-Cr**	**LM-In**	**LM-Cr**	**SM-In**	**SM-Cr**
	Wet				**LS**				**Wet**			
Day 1	n.s.	n.s.	n.s.	n.s.	**Dry****	**Dry***	**Dry***	**Dry****	n.s.	n.s.	n.s.	n.s.
Day 2	n.s.	n.s.	n.s.	n.s.	**Dry****	**Dry***	n.s.	**Dry****	n.s.	n.s.	n.s.	n.s.
Day 6	n.s.	n.s.	n.s.	n.s.	**Dry***	n.s.	n.s.	**Dry****	n.s.	n.s.	n.s.	n.s.
Day 9	n.s.	n.s.	n.s.	n.s.	**Dry****	n.s.	n.s.	**Dry****	n.s.	n.s.	n.s.	n.s.
Day 13	n.s.	n.s.	n.s.	n.s.	**Dry***	n.s.	**Dry***	**Dry****	n.s.	n.s.	n.s.	n.s.
Day 20	n.s.	n.s.	n.s.	n.s.	**Dry***	n.s.	**Dry***	**Dry****	n.s.	n.s.	n.s.	n.s.
Day 28	n.s.	**AS***	n.s.	n.s.	**Dry****	n.s.	**Dry***	**Dry****	n.s.	n.s.	n.s.	n.s.
Day 48	n.s.	n.s.	n.s.	n.s.	**Dry****	**Dry***	**Dry***	**Dry****	n.s.	n.s.	n.s.	n.s.
Day 76	n.s.	n.s.	n.s.	n.s.	**Dry****	**Dry***	**Dry***	**Dry****	n.s.	n.s.	n.s.	n.s.
	Dry				**AS**				**Dry**			
Day 1	**LS***	n.s.	**LS***	n.s.	n.s.	n.s.	n.s.	n.s.	n.s.	n.s.	n.s.	n.s.
Day 2	**LS***	**LS***	**LS***	n.s.	n.s.	n.s.	n.s.	n.s.	n.s.	n.s.	n.s.	n.s.
Day 6	**LS***	n.s.	n.s.	**LS***	n.s.	n.s.	n.s.	n.s.	n.s.	n.s.	n.s.	**A***
Day 9	**LS***	n.s.	n.s.	**LS***	n.s.	n.s.	n.s.	n.s.	n.s.	n.s.	n.s.	**A***
Day 13	n.s.	n.s.	**LS***	**LS****	n.s.	n.s.	n.s.	n.s.	n.s.	n.s.	n.s.	**A****
Day 20	n.s.	**LS***	n.s.	**LS***	n.s.	n.s.	n.s.	n.s.	n.s.	n.s.	n.s.	**A***
Day 28	n.s.	n.s.	n.s.	**LS****	n.s.	n.s.	n.s.	n.s.	n.s.	n.s.	n.s.	**A****
Day 48	n.s.	**LS***	n.s.	**LS****	n.s.	n.s.	n.s.	n.s.	n.s.	n.s.	n.s.	**A****
Day 76	n.s.	**LS***	n.s.	**LS****	n.s.	n.s.	n.s.	n.s.	n.s.	n.s.	n.s.	**A****

LS: limestone soil, AS: acid igneous rock soil, LM: large macroaggregates (>2 mm), SM: small macroaggregates (0.25-2 mm), MA: macroaggregates (>0.25 mm), A: A horizon, In: aggregate intact, Cr: aggregate crushed, Wet: the wet site, Dry: the dry site, *: P<0.05 **: P<0.01, n.s.: not significant.

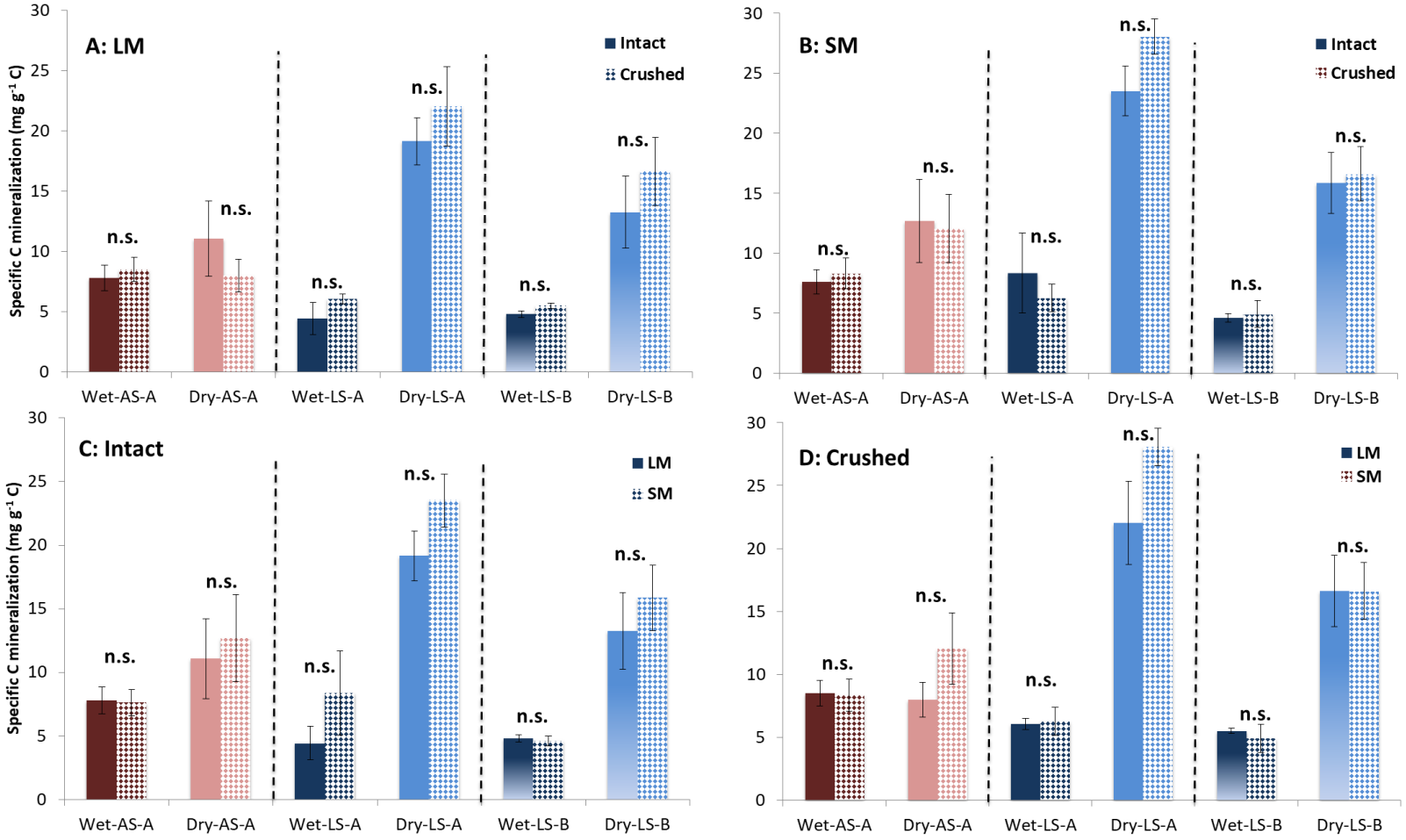

Fig. 6 Effects of aggregate destruction and aggregate size on specific SOC mineralization rates in the sampling day 76 (Mean ± SE). A: comparing aggregates intact and crushed in large macroaggregates, B: comparing aggregate intact and crushed in small macroaggregates, C: comparing large and small aggregates with aggregates intact, D: comparing large and small aggregates with aggregates crushed. LS: limestone soil, AS: acid igneous rock soil, LM: large macroaggregates (>2 mm), SM: small macroaggregates (0.25-2 mm), Intact: incubation with aggregates intact, Crushed: incubation with aggregates crushed, A: A horizon, Wet: the wet site, Dry: the dry site, n.s.: not significant.

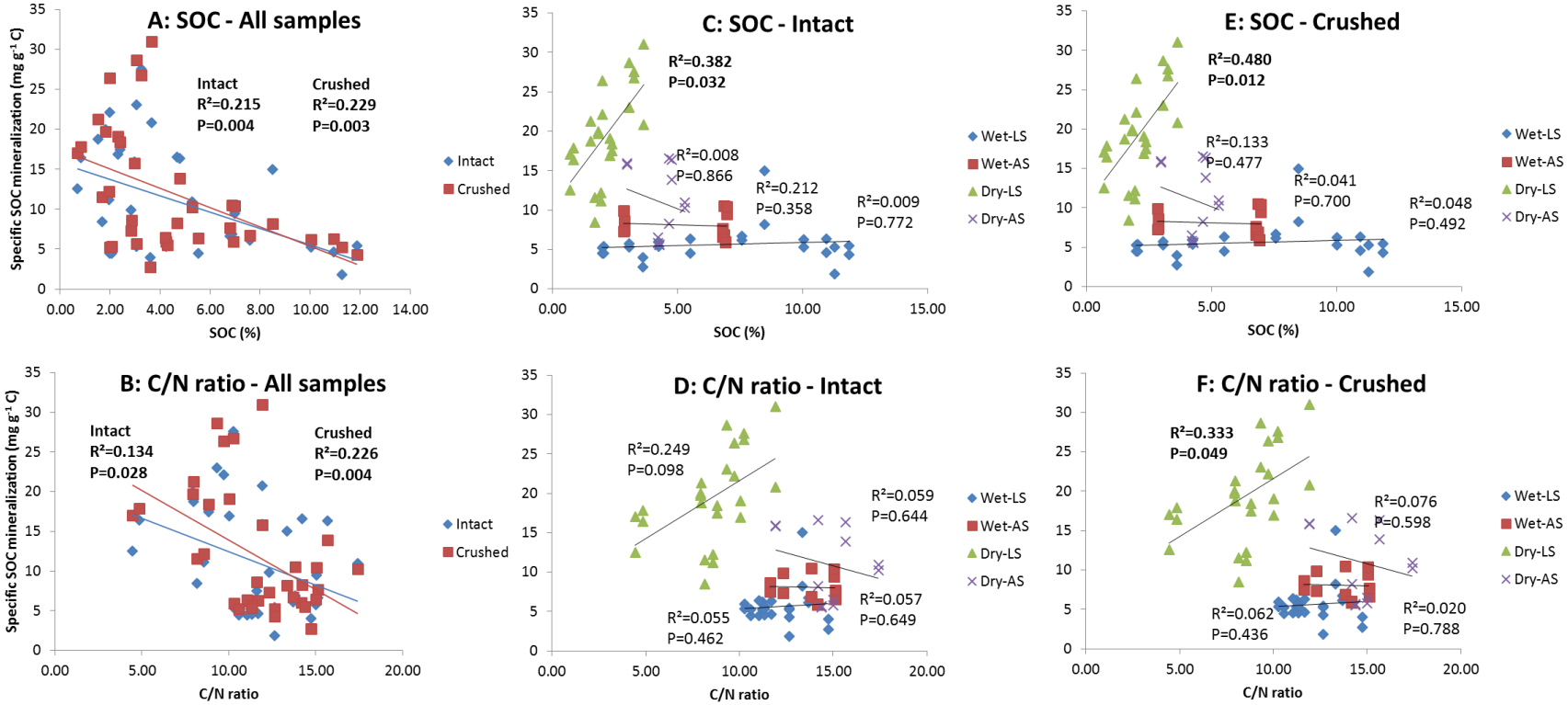

Fig. 7 Relationships of specific C mineralization rates (Day 76) with organic carbon contents and C/N ratios when soil aggregates were intact and crushed. Wet: the wet site, Dry: the dry site, LS: limestone soil, AS: acid igneous rock soils, SOC: soil organic carbon content.